Available online at www.sciencedirect.com
ScienceDirect
Journal of the European Ceramic Society 31 (2011) 2037–2042
www.elsevier.com/locate/jeurceramsoc

Ring-on-ring testing of thin, curved bi-layered materials

G. Pećanac, T. Bause, J. Malzbender *

Forschungszentrum Jülich GmbH, IEK-2, 52428 Jülich, Germany

Received 22 February 2011; received in revised form 21 April 2011; accepted 16 May 2011

Abstract

The bi-axial ring-on-ring test is a convenient method to determine elastic modulus and fracture strength of brittle materials in plate geometry. However, standard analytical relationships appear to be limited to flat isotropic samples with discrete ratios of thickness to loading/support ring radii. In addition to the necessity to consider residual stresses due to differences in thermal expansion for bi-layered materials, the curvature of thin components complicates the analysis of the experimental data. Experimental and finite element modeling results are presented for thin curved bi-layered materials with substrates of different elastic behavior. Basis for the analysis are experimental results obtained for solid oxide fuel cells with anode substrates in oxidized and reduced state. A testing procedure and its limits are outlined that permits to extend the use of standard analytical relationships to curved bi-layered specimens with the aim to determine the properties of the mechanically dominating support material.

Keywords: C. Fracture; C. Strength; Elastic behavior; Solid oxide fuel cells; Bending test

1. Introduction

The mechanical properties of isotropic ceramic materials in plate geometry can be conveniently assessed using ring-on-ring bending tests.[1] For brittle materials the test permits to calculate both elastic modulus and fracture stress.[2] Furthermore, statistical analysis of the fracture stress data allows a determination of a characteristic strength and the Weibull modulus, which are parameters that can be used to determine tolerable stress limits for a given failure probability.[3] However, theories to determine the stress state and stiffness values from the experimental load–displacement curve appear to be limited to isotropic materials and require a discrete ratio of specimen thickness to loading/support ring ratio.[1,2] The analytical approach is also limited to deflections significantly smaller than the specimen thickness which restricts the applicability of the test. In fact, the critical deflection depends on the ratio of the radii of the loading to supporting ring and takes a value of ~50% of the specimen thickness for a support ring to loading ring ratio of two.[2,4]

Another complication with the ring-on-ring test arises when a statistical evaluation of the results is requested. The statistical analysis requires a determination of characteristic strength and Weibull modulus. However, the strength value decreases with increasing deformed characteristic area/volume.[2,3,6] Linear bending theory is only valid if the deflection of planar specimen does not exceed a discrete value. At large deflections the fracture will no longer start from the central sample region.[4] Due to the local stress arising just opposite to the loading ring an ill defined characteristic area/volume is obtained hence a determination of the stress localization at larger deflections is necessary.

Further complications arise, if tests are carried out with thin layered functional ceramics, since differences in thermal expansion of the layers can result in warpage and residual stresses.[5–7] Solid oxide fuel cells (SOFCs) and gas separation membranes are examples of bi-layered brittle ceramic materials which are typically applied in energy conversion technologies.

In the current work solutions based on FEM analyses for curved bi-layered materials are presented. The analysis of the data also permits to assess through-thickness stress gradients. The results are compared with the experimentally obtained bending behavior of bi-layered, curved SOFC samples. The results should provide a basis to derive a testing methodology that can be applied to a wider range of functional layered ceramic materials.

The manuscript clearly shows the limits of analytical approaches, however, also verifies that analytical relationships can still be used for bi-layered materials with initial curvature using an appropriate analysis procedure. To determine the elastic properties of the mechanically dominating substrate material

* Corresponding author. Tel.: +49 2461616964; fax: +49 2461613699.
E-mail address: j.malzbender@fz-juelich.de (J. Malzbender).

0955-2219/$ – see front matter © 2011 Elsevier Ltd. All rights reserved.
doi:10.1016/j.jeurceramsoc.2011.05.021

a FEM analysis is not necessary since an appropriate deflection range can be chosen. Fracture of high strength materials might occur in a range where the analytical relationships are not valid anymore. All limitations can be avoided using an FEM based analysis which can be used to predict stresses even for the non-linear behavior of warped bi-layered materials.

2. Experiments

SOFC half-cell samples supplied by CeramTec GmbH (Marktredwitz, Germany) have been investigated in the present work. These planar SOFCs consist of an anode substrate that provides the mechanical support for the electrolyte layer. For anode supported SOFCs usually the electrolyte is at least one order of magnitude thinner than the substrate. In the as-sintered state, the anode substrate consists of Nickel oxide (NiO) and yttrium-stabilized zirconia. The electrochemical operation requires NiO to be reduced to Ni. Due to the thermal expansion mismatch of substrate and electrolyte layer ($\Delta\alpha \sim 2 \times 10^{-6}\,K^{-1}$),[9] an unconstrained half-cell composite bends progressively towards the free surface of the anode during the cool down to RT. Note that the reduction of NiO to Ni leads to an additional change in substrate stiffness which is reflected in an curvature increase.[8]

The half-cell samples were tested here under bi-axial loading in a ring-on-ring test arrangement that avoids contrary to conventional three- or four-point bending the failure due to edge damage (flaws) resulting from preparation/cutting flaws.[9] The specimens were supported by an outer ring ($r_2 \sim 9.5$ mm) and loaded with a smaller coaxial inner ring ($r_1 \sim 4.5$ mm). The circular disk samples ($r_3 \sim 12.55$ mm) were loaded with a rate of 100 N/min at room temperature in oxidized and reduced anode state, respectively. The samples had an overall thickness of ~310 μm (anode substrate layer ~300 μm, electrolyte layer ~10 μm). During the reduction of the samples (4% H_2/Ar) the radius of curvature of the specimens changed from ~520 mm to ~170 mm.

To test the effect of positioning, either the electrolyte layer (the composite has a concave shape with respect to the loading ring) or the free surface of the substrate layer (the composite has a convex shape, Fig. 1) was placed on the support ring. The finite element analysis was carried out using the ANSYS© software package. Simulation was made in 2D axis-symmetry using 2D 8-node elements (PLANE183). The loading and supporting rings were approximated with line loads and line supports. The load was applied on one node as the change in loading contact position due to bending showed small influence and thus was neglected. Geometry and material properties were taken from experimental data and used as input data for the simulation. Although the materials were assumed to be linear elastic, non-linear behavior was taken into consideration using the appropriate large deflection settings of the program. It has been verified in literature 2 that the influence of the friction can be neglected.

3. Analytical relationship

In the following the linear elastic analytical relationships to assess stress/deflection behavior using ring-on-ring bending test are briefly summarized. According to the linear bending theory the maximum surface stress for a flat plate is[2]:

$$\sigma_b = \frac{3 \cdot F \cdot (1+\nu)}{2 \cdot \pi \cdot t^2} \cdot \left(In\frac{r_2}{r_1} + \frac{1-\nu}{1+\nu} \cdot \frac{r_2^2 - r_1^2}{2 \cdot r_3^2} \right) \quad (1)$$

where ν is the Poisson's ratio, F is the applied force, t is the specimen thickness, and r_1, r_2 and r_3 are radii of the loading ring, supporting ring and specimen, respectively. The maximum tensile stress arises opposite to the loading ring. However, the relationship gives accurate results only for deflections that are smaller than around half the specimen thickness for $r_2/r_1 = 2$. Note that the validity of the relationship is increased to around three times the specimen deflection if $r_2/r_1 = 5$. At large deflections, in the non-linear state, a progressively increasing difference between the really existing and analytically predicted stress distribution exists.

Linear elastic theory also links central specimen deflection u and elastic modulus E[2]:

$$u = \frac{3 \cdot F \cdot (1-\nu^2)}{2 \cdot \pi \cdot E \cdot t^3} \cdot \left(r_2^2 + \frac{r_2^2 \cdot (1-\nu) \cdot (r_2^2 - r_1^2)}{2 \cdot (1+\nu^2) \cdot r_3^2} \right) - r_1^2 \cdot \left(1 + In\left(\frac{r_2}{r_1}\right) \right) \quad (2)$$

However, for bi-layered material the flexural rigidity will change due to the presence of an additional layer and the term for a single layer $I = E\,t^3/12$ which is part of Eq. (2) has to be replaced by $I_2 = (E_s^2 \cdot t_s^4 + E_c^2 \cdot t_c^4 + 2 \cdot E_s \cdot E_c \cdot t_s \cdot t_c \cdot (2 \cdot t_s^2 + 3 \cdot t_s \cdot t_c + 2 \cdot t_c^2)/(12 \cdot (E_s \cdot t_s + E_c \cdot t_c))$ [6,10]. The presence of the 10 μm thin electrolyte (YSZ, $E_C = 200$ GPa, $\nu = 0.3$ at RT) makes the half-cell stiffer, yielding a ~15% lower deflection for the composite with oxidized anode in comparison with a monolithic oxidized anode substrate. This is also supported by FEM results. Hence, the effect of the layer cannot be

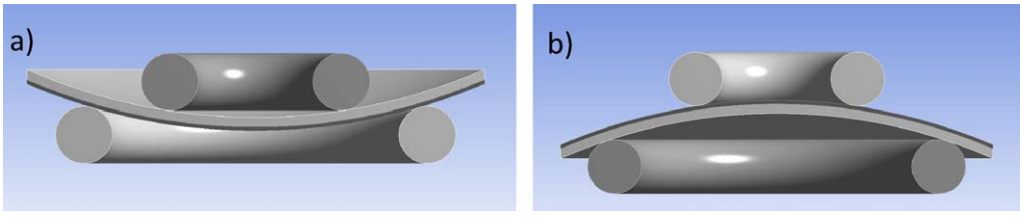

Fig. 1. Definition of the (a) concave and (b) convex bending direction.

neglected. The multiplication factor to be included in Eqs. (1) and (2) is:

$$f_1 = \frac{I_2}{I} \tag{3}$$

In addition to the change in bending stiffness due to the layer the change in neutral axis needs to be considered in the calculation of the fracture stress. However, for a coating with an elastic modulus of twice the substrate value the effect is rather small, ~5% for a relative coating thickness of 2.5% and ~10% for a relative coating thickness of 5%. Hence for thin coatings this effect can be neglected. To determine the stress additional corrections are necessary. The change in the neutral axis can be included in Eq. (2) by the term:

$$f_2 = \frac{t_s/2}{t_n} = \frac{t_s/2}{(E_s \cdot t_s^2 - E_c \cdot t_c^2)/2 \cdot (E_s \cdot t_s + E_c \cdot t_c)} \tag{4}$$

Furthermore, for a bi-layered material with differences in thermal expansion the total stress is the sum of applied and residual stress. The residual stresses resulting from differences in thermal or chemical expansion mismatch (in terms of an equivalent thermal expansion difference $\Delta\alpha = \Delta\varepsilon/T$) can be calculated analytically based on the temperature dependency of the thermal expansion and all material properties, relationships for the substrate stress at the free surface and near the coating interface are given in Ref. 11. A relationship to determine the electrolyte stress from the room temperature curvature has been derived in Ref. 8. The stress changes linear across the substrate. If the room temperature curvature is known than the residual stress in the substrate at the free surface and near the interface with the layer can be determined from the room temperature properties using:

Substrate residual stress-free surface :

$$\sigma_{Rf} = -\frac{1}{6r}(3E_s t_c + 4E_s t_s) \tag{5}$$

Substrate residual stress-interface :

$$\sigma_{Ri} = \left(-\frac{1}{6r}(-3E_s t_c - 2E_s t_s)\right) \tag{6}$$

where r is the radius of curvature of the sample which can be easily obtained experimentally. Higher order terms were neglected in these relationships. The resulting error is equivalent to the relative coating thickness, being for example for a coating thickness of 3% of the substrate thickness 3%, for a relative thickness of 10% the error is 10%. The advantage of the approach is that similar as in Eqs. (1) to (4) only room temperature properties are necessary to determine the residual stress. It is important to note that knowledge of the stress free temperature and the temperature dependency of the thermal expansion coefficients and elastic moduli is not necessary.

Based on the analytical results the following procedure can be suggested: First step is to correct the elastic modulus and fracture stress for the change in flexural rigidity and neutral axis induced by the additional layer (leading to a decrease in deflection and stress at a particular load). Second step is to add/subtract the residual stress, which is the main influence factor. The correct relationship for the stress is therefore:

$$\sigma_s = (\sigma_b \times f_1 \times f_2) + \sigma_R \tag{7}$$

where the term σ_R depends on the bending direction, i.e. whether the substrate free surface or the interface is under the tensile bending stress. For the deflection of the composite the respective relation is:

$$u_s = (u \times f_1) \tag{8}$$

A curvature of 520 mm for a half-cell with oxidized anode is associated with a compressive stress of ~−31 MPa at the free substrate surface, while close to the electrolyte interface the substrate stress is ~66 MPa. Contrary to the concave plate direction, for bending in the convex plate direction the residual stress counteracts the bending stresses.

Hence elastic modulus and fracture stress can be determined for a composite material using Eqs. (7) and (8); however the question to be answered in the following is: what are the limits of the approach outlined above for of thin curved bi-layered materials.

4. Results and discussion

First, the anode substrate without electrolyte coating was simulated as flat isotropic plate with a thickness of 300 μm. For the elastic modulus and Poison's ratio typical values for NiO-YSZ SOFC anode at RT were used ($E = 115$ GPa, $\nu = 0.3$). The radius of specimen, loading and supporting ring are given in the experimental section. The resulting displacement– and stress–load dependencies show the expected difference in behavior between analytical (Eqs. (1) and (2)) and non-linearity FEM solution at larger deflections (Fig. 2a and b). Obviously the thin plate exhibits non-linear behavior when deflection exceeds ~½ thickness and the specimen becomes stiffer and the deflection is significantly smaller than predicted by the analytical solution. When the deflection approaches the specimen thickness the tensile stress is not homogenous anymore, giving rise to a peak stress just opposite the loading ring (Fig. 2b, insert).

If a flat anode substrate with coating is considered the FEM result reveals a similar behavior as for the uncoated substrate, the only difference is that the slope of the curves will be changed due to the larger stiffness of the composite in agreement with the predictions of the analytical approach (Eqs. (7) and (8)) outlined above.

If the same composite sample is already curved before the test and placed between the loading and supporting ring in a way that the curvature is increased by the applied load (Fig. 1a, concave plate) the composite shows non-linear behavior already at significantly smaller deflections of ~¼ of the total thickness (Fig. 3a). The FEM result is in good agreement with the experimentally obtained displacement–load curve. Only the substrate near the coating interface has to be considered as the failure relevant position, since the coating will be under compressive stresses of a few hundred MPa. The residual stress adds to the applied bending stress, hence the stress–load curve does not go through zero (Fig. 3b). Much smaller stresses are obtained than

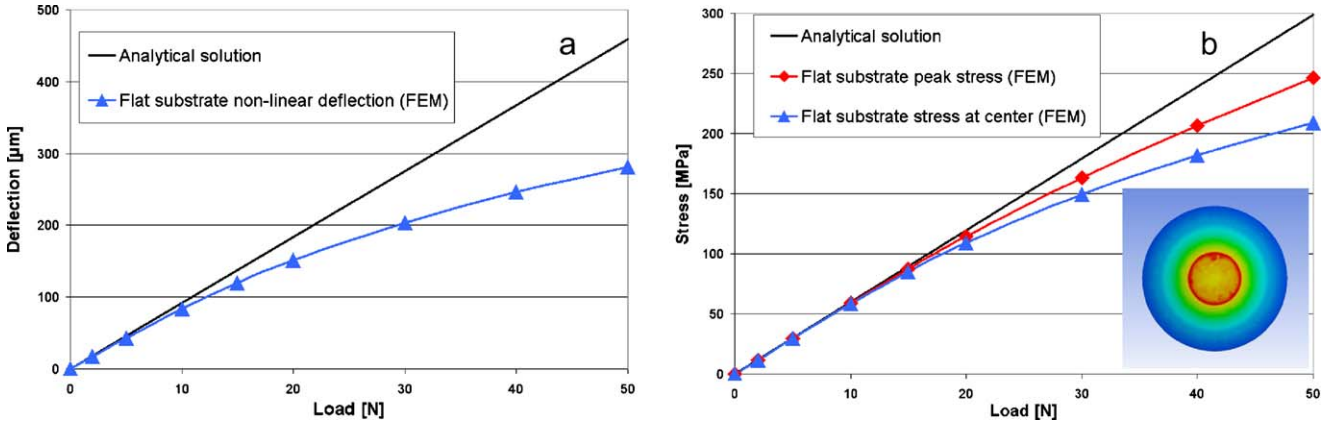

Fig. 2. Comparison of analytical and FEM result for the (a) deflection– and (b) stress–load behavior for a flat plate. Insert shows the stress localization of the in-plane surface tensile stress for large deflections.

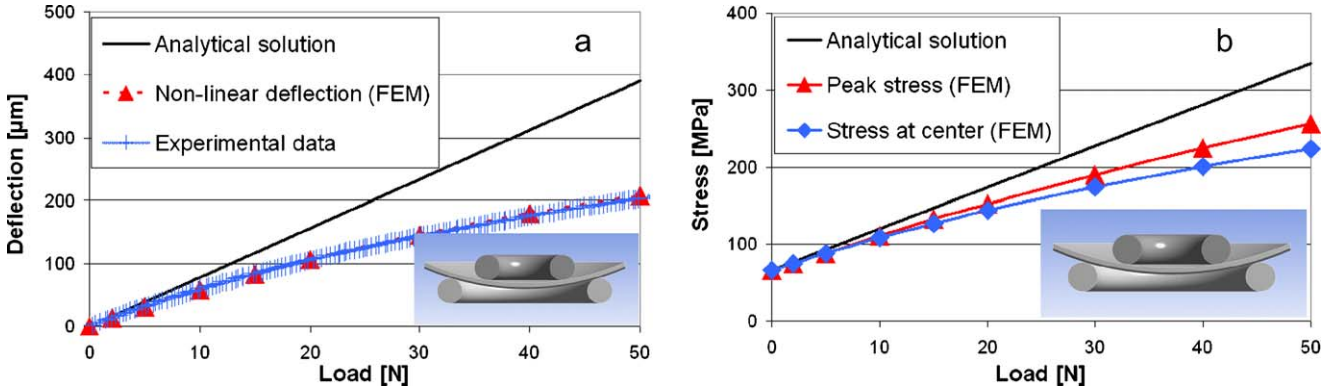

Fig. 3. Comparison of analytical and FEM result for the (a) displacement–load and (b) stress–load dependencies for the concave-shape.

in the analytical approach (Eqs. (7) and (8)), the curves diverge at much smaller deflections than ~½ of the thickness. Again a local peak stress arises in the surface opposite to the loading ring at larger deflections.

For the bi-layered composite plate which is curved initially in the so-called convex direction the curvature that results from difference in thermal expansion is reduced during the test (Fig. 1b). The sample becomes initially more flat and is then bended in the opposite direction (Fig. 4a). Again the FEM result is in good agreement with the experimentally obtained displacement–load curve. Analytical and FEM result agree up to a deflection of ~¾ of the specimen thickness, a larger value than for flat plate and concave bending. Here the compressive residual stress counteracts the bending stress (Fig. 4b). Even at deflections equal the specimen thickness (load 50 N) analytical (Eqs. (7) and (8)) and FEM result show close agreement (difference < 10%). A more uniform stress distribution is obtained since the peak stress in the large deflection regime is reduced. Hence, this bending direction

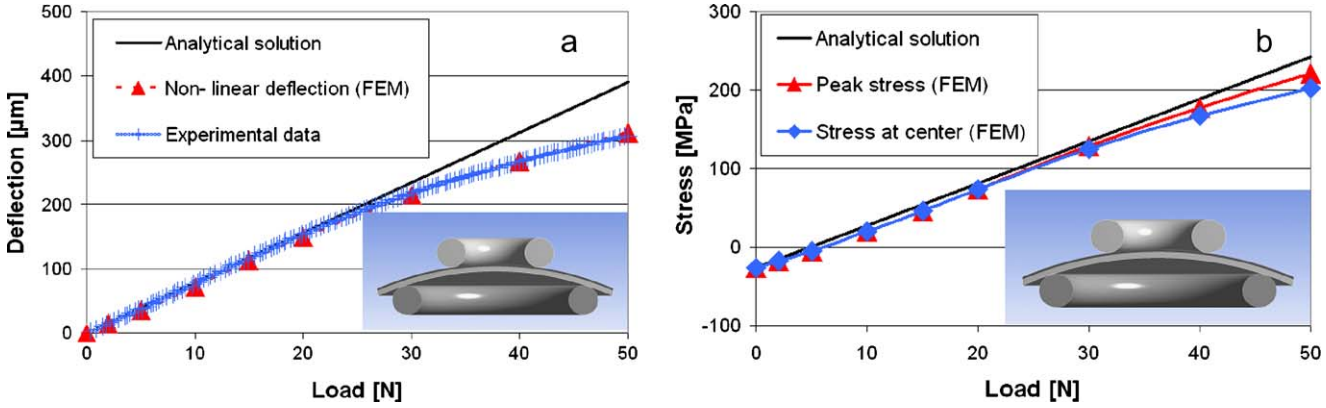

Fig. 4. Comparison of analytical and FEM result for the (a) displacement–load and (b) stress–load dependencies for the convex-shape.

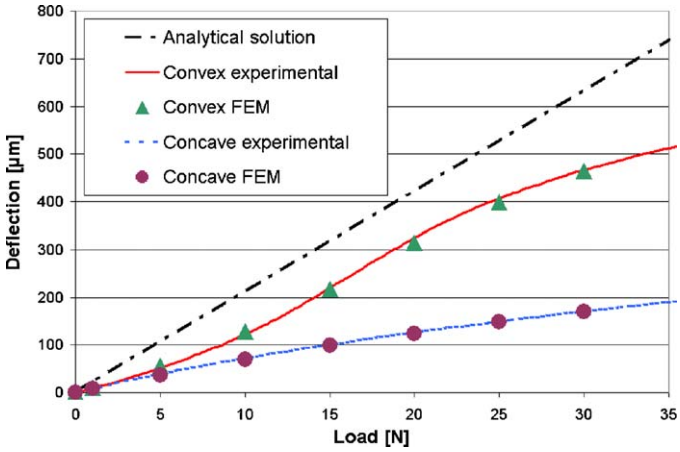

Fig. 5. Comparison of analytical and FEM result for the displacement–load dependence for different materials and geometry shapes.

is preferable, permitting an analytical determination of elastic modulus and stress in an even larger deflection range than for flat plates.

The anodes of the half-cells can be in an oxidized (NiO-YSZ) or reduced (Ni-YSZ) state. Oxidized and reduced anode have shown differences in elastic modulus (∼35 GPa reduced, 115 GPa oxidized) and radius of curvature (∼170 mm reduced, 520 mm oxidized). These data permit a test of the effect of the substrate stiffness and specimen curvature on the mechanical behavior of the composite specimens in a ring-on-ring bending test. Lower elasticity and larger curvature should affect displacement– and stress–load behavior.

Again FEM result agrees well with the experimentally obtained displacement–load behavior for both initially convex as well as concave bending direction (Fig. 5). Due to the larger initial curvature of the reduced samples a larger difference is obtained between analytical (Eqs. (7) and (8)) and FEM result in both bending directions (Figs. 5 and 6, residual stresses are not considered in these plots). As expected, the concave plates exhibit the larger difference to the analytical approach since initial deflection and bending induced deflection superimpose.

Additional simulations for the initially convex direction were carried out for an oxidized NiO-YSZ specimens with a larger initial curvature ($r \sim 170$ mm), which is equivalent to that of a reduced Ni-YSZ specimen at RT, and a reduced specimen with an initial smaller curvature, being equivalent to that of an oxidized specimen ($r \sim 520$ mm, similar to the state of the reduced specimens at ∼800 °C). The results presented in Fig. 7 show that for large initial curvature of an oxidized specimen an analytical description of the deformation–load behavior is not possible anymore even for small initial bending deflections, whereas the

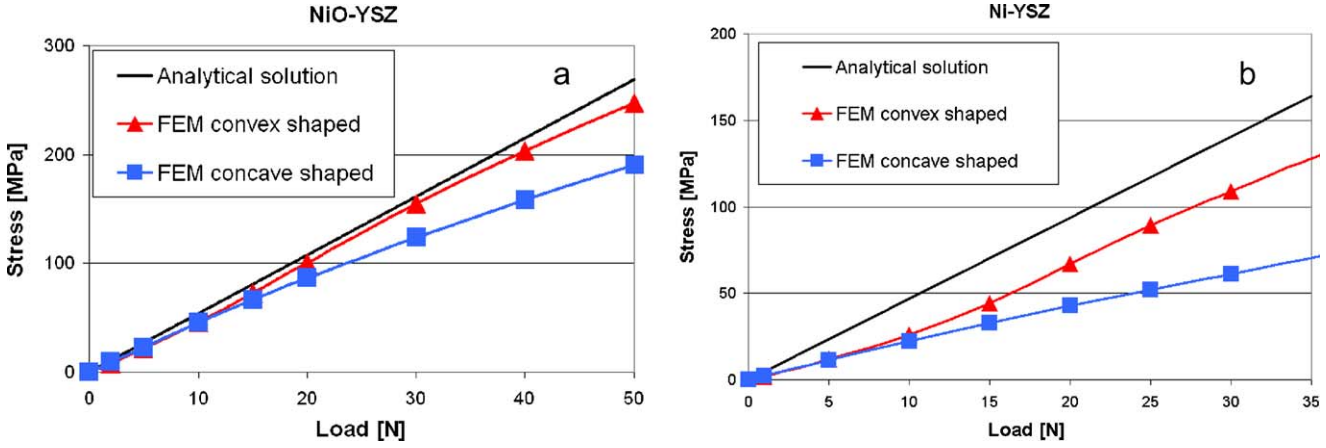

Fig. 6. Comparison of stress state for different materials and geometry shapes.

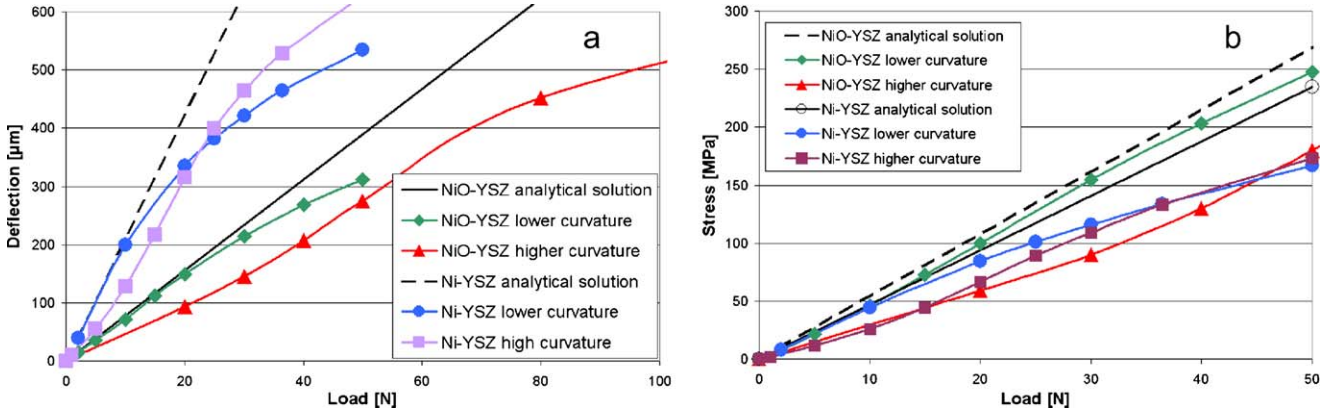

Fig. 7. Initial curvature influence on (a) displacement–load and (b) stress–load dependencies.

reduced specimen with a small initial curvature can be described by the analytical relationship up to a deflection of almost its thickness.

5. Conclusions

FEM results were compared to analytical predictions for the bending behavior of curved bi-layered material composites with a thin top layer in a ring-on-ring test. In general changes in flexural rigidity, neutral axis as well as residual stresses due to thermal mismatch need to be taken into consideration. Simple relationships are given to assess the stress state in the substrate materials based on the room temperature curvature. However, for asymmetric layered specimens the residual stress is also associated with warping which influences the bending behavior. Hence, the direction of warping with respect to the applied loading direction is important. The results clearly show that the ring-on-ring bending test with the specimen initially in the convex direction is preferable. This orientation permits the use of the analytical relationships to an even larger deflection than for a flat plate under identical boundary conditions. However, independent of the substrate stiffness the approach is limited to a small initial radius of curvature (∼170 mm).

The elastic modulus can be determined analytically up to a deflection of approximately ¾ the specimen thickness. The analytical approach can be used to determine the fracture stress up to a deflection equal the specimen thickness for the NiO-YSZ composite. For the Ni-YSZ substrate of identical initial curvature the range is narrowed and at a deflection of 1.5 times the initial thickness a difference of 30% to the analytical solution is obtained. The presented plots can serve as a tool to assess the elastic modulus and fracture stress also at larger deflections and for large initial curvatures where the analytical approach is not valid anymore.

Although in general FEM based procedures are very valuable they are not always available and the analysis of materials data has often to be based on analytical procedures. The current work clearly verifies that for the rather complex case of the bending of bi-layered materials with initial curvature an analytical procedure is possible. For very precise analysis and especially in complex cases, FEM simulations should be used. The analytical approach can be extended to multilayer materials using the appropriate relationships for the residual stress, flexural rigidity and position of the neutral axis.

Acknowledgements

The author would like to thank CeramTec GmbH, Marktredwitz, Germany for providing the half-cells material. The research leading to these results was partly funded by the European Union's Seventh Framework Programme FP7/2007-2013 under grant agreement n° 228701.

References

1. Bestimmung der Biegefestigkeit, *Deutsche Norm* DIN 52292 Teil 1; 1984.
2. Morrell R. Biaxial flexural strength testing of ceramic materials. *Measurement good practice guide No. 12*; 1998.
3. Giovan MN, Sines G. Biaxial and uniaxial data for statistical comparisons of ceramic's strength. *J Am Ceram Soc* 1979;**62**(9–10):510–5.
4. Kao R, Perrone N, Capps W. Large- deflection solution for the coaxial-ring circular-glass-plate flexure problem. *J Am Ceram Soc* 1971;**54**:566–71.
5. Selçuk A, Atkinson A. Strength and toughness of tape-cast yttria-stabilized zirconia. *J Am Ceram Soc* 2000;**83**(8):2029–35.
6. Malzbender J, Steinbrech RW. Fracture test of thin sheet electrolytes for solid oxide fuel cells. *J Eur Ceram Soc* 2007;**27**:2597–603.
7. Malzbender J, Steinbrech RW. Substrate stiffness determination in curved layered composites using bending methods. *Surf Coat Technol*, **202**(2):379–81.
8. Malzbender J, Fischer W, Steinbrech RW. Studies of residual stresses in planar solid oxide fuel cells. *J Power Sources* 2008;**182**(2):594–8.
9. Malzbender J, Steinbrech RW. Threshold fracture stress of thin ceramic components. *J Eur Ceram Soc* 2008;**28**(1):247–52.
10. Hsueh CH, Thompson GA, Jadaan OM, Wereszczak AA, Becher PF. Analyses of layer-thickness effects in bilayered dental ceramics subjected to thermal stresses and ring-on-ring tests. *Dent Mater* 2008;**24**(1):9–17.
11. Hsueh C-H. Some considerations of determination of residual stresses and Young's moduli in ceramic coatings. *J Am Ceram Soc* 1991;**74**(7):1646–9.